Bihari, Nupur; Heikkinen, Ismo T. S.; Marin, Giovanni; Ekstrum, Craig; Mayville, Pierce J.; Oberloier, Shane; Savin, Hele; Karppinen, Maarit; Pearce, Joshua

Vacuum Outgassing Characteristics of Unpigmented 3-D Printed Polymers Coated with ALD Alumina

Published in:
Journal of Vacuum Science and Technology A: Vacuum, Surfaces and Films

DOI:
10.1116/6.0000178

Published: 01/09/2020

Document Version
Peer-reviewed accepted author manuscript, also known as Final accepted manuscript or Post-print

Please cite the original version:
Bihari, N., Heikkinen, I. T. S., Marin, G., Ekstrum, C., Mayville, P. J., Oberloier, S., Savin, H., Karppinen, M., & Pearce, J. (2020). Vacuum Outgassing Characteristics of Unpigmented 3-D Printed Polymers Coated with ALD Alumina. *Journal of Vacuum Science and Technology A: Vacuum, Surfaces and Films*, *38*(5), Article 053204. https://doi.org/10.1116/6.0000178

Vacuum Outgassing Characteristics of Unpigmented 3-D Printed Polymers Coated with ALD Alumina

Nupur Bihari[1§], Ismo T. S. Heikkinen[2§], Giovanni Marin[3§], Craig Ekstrum[1], Pierce J. Mayville[1], Shane Oberloier[4], Hele Savin[2], Maarit Karppinen[3] and Joshua M. Pearce[1,2,4a)]

1. Department of Materials Science & Engineering, Michigan Technological University, Houghton, MI USA.

2. Department of Electronics and Nanoengineering, School of Electrical Engineering, Aalto University, Espoo, Finland.

3. Department of Chemistry and Materials Science, School of Chemical Engineering, Aalto University, Espoo, Finland.

4. Department of Electrical & Computer Engineering, Michigan Technological University, Houghton, MI USA.

[§]These authors contributed equally to this manuscript.

[a)]Email: pearce@mtu.edu

Abstract

3-D printing offers enormous potential for fabricating custom equipment for space and vacuum systems, but in order to do this at low-costs, polymers are necessary. Historically polymers have not been suited for these applications because of outgassing, but if coated with a conformal, inorganic film introduced with atomic layer deposition (ALD), then outgassing can be reduced. Previous work on coating ALD layers showed promise with heavily outgassing carbon black

containing 3-D printed polymers. In this study, ALD aluminum oxide and a commercially available vacuum sealant resin were used to coat clear, acrylonitrile butadiene styrene (ABS), polycarbonate (PC) and polypropylene (PP). Characterization of the films included spectroscopic ellipsometry for thickness, microstructure analysis with scanning electron microscopy, chemical analysis with energy-dispersive X-ray spectroscopy, and residual gas analysis to study relative change in outgassing. ALD-coated samples registered lower pressures than the resin-coated ones. The results showed that the ALD coatings could effectively inoculate unpigmented 3-D printed plastics, which could be used in contamination-sensitive environments such as semiconductor processing systems and space environments.

Keywords: clean room; vacuum; outgassing; polymer; atomic layer deposition; semiconductor processing

I. INTRODUCTION

Additive manufacturing is radically changing the way polymer-based components are manufactured[1-5], which enables the customization of 3-D printed components to meet individual user needs. Customization with 3-D printing has significantly reduced costs and led to unprecedented growth in the acceptance and use of polymers in scientific research equipment[6-9]. 3-D printed parts allow for versatile design and manufacture of custom parts at relatively low expense by low to moderately skilled workers[10-12] and a high return on investment for labs that deploy them[13]. Despite the ubiquity of 3-D printed materials in research applications, including recent inroads into clean room environments[14-15]; they have remained largely absent from

semiconductor research, primarily due to their apparent incompatibility with vacuum equipment. This assumed incompatibility arises from off-gassing of polymers when exposed to vacuum conditions, chemical degradation driven by exposure to charged and high kinetic energy particles, as well as ultraviolet radiation used in some semiconductor processing systems.

The conditions experienced in vacuum systems for semiconductor processing are akin to those seen in space, where polymers degrade under exposure to ultrahigh vacuum, ultraviolet radiation, charged particles (plasma, electrons, protons), and atomic oxygen[16-19]. Mechanical degradation manifests as embrittlement of the material by initiation of stress concentrators by polymer decomposition, which can cause failure when polymer parts are under thermal cycling or tensile loads[20-22]. In addition to absorption and desorption of water, off-gassing in polymers arises from the low molecular weight molecules present in the material matrix (e.g. unreacted monomers, solvents, plasticizers, antioxidants, coloring agents, and other processing aids are all common in commercial polymer material). When introduced to vacuum conditions, these low molecular weight species, known as volatile organic compounds (VOCs) outgas[23-26]. This outgassing may result in lowered robustness through accelerated photo-degradation reactions in the polymer, as well as contamination of the surrounding system[27].

If polymers are coated with a conformal, inorganic film introduced with atomic layer deposition (ALD), outgassing can be reduced to a large extent, because the surface layer acts as a seal to prevent low molecular weight species present in the bulk of the material from escaping. This method of using ALD coatings as gas barriers[28-29] is known in the packaging industry, where aluminum oxide (AlO_x) and silicon oxide films are used as barrier layers to achieve relatively impermeable polymer-based structures[30-31], as well as with OLED encapsulation[32-34]. This work lays a strong foundation showing that transmission rates of volatiles through ALD coated

polymers can be decreased immensely; supporting the potential for the application of 3-D printed polymer parts in vacuum systems and in space environments.

In addition to providing a barrier to volatile gas transmission, ALD layers have been shown to protect polymer layers from ionizing radiation and high kinetic energy particles[35]. The deposition of inorganic coatings on 3-D printed parts has the potential to seal air pockets and reduce the number of stress concentrators that lead to part failure[36-37]. Such stress concentrators may be formed due to particle impingement on either coated or uncoated components[38]. This research aims to understand the relative outgassing characteristics of 3-D printed polymers with ALD coatings and evaluate the efficacy of the coating in protecting the underlying polymer against very high vacuum (10^{-6} to 10^{-7} Torr), the most commonly seen ambient condition in semiconductor processing systems, and in space.

To limit gas diffusion in 3-D printed components, ALD AlO_x and a commercially available vacuum sealant resin, Vacseal[39], were chosen as potential coatings on clear, unpigmented acrylonitrile butadiene styrene (ABS), polycarbonate (PC) and polypropylene (PP). Previous research by the group using black colored ABS and PC[40] determined that relative outgassing is high when carbon black is used as pigment[41]. While an inorganic ALD coating on black polymer was successful in minimizing outgassing, the effects of using clear, unpigmented polymeric materials (and thus no artificially-enhanced outgassing) with these coatings are studied here. Characterization included spectroscopic ellipsometry for film thickness, microstructure analysis with scanning electron microscopy (SEM), chemical analysis with energy-dispersive X-ray spectroscopy (EDS), and residual gas analysis for relative outgassing quantification. This vacuum outgassing characterization is an important initial step for selecting a material that will

be used to create open-source 3-D printable components, which could be used in contamination-sensitive environments such as semiconductor processing systems and space.

II. EXPERIMENTAL

Three types of clear, unpigmented materials were studied: acrylonitrile butadiene styrene (ABS), polycarbonate (PC) and polypropylene (PP). ABS was chosen because of its wide availability and ease of use[42], PC for its strength and thermal stability[43-45], and PP for its chemical inertness[46]. The selected polymers exhibit a low percentage of total mass loss (TML): 0.94, 0.12 and 0.23 for ABS, PC and PP respectively.[47]. 3-D printed samples of the materials were coated with either ALD AlO_x or a commercial sealant, and their microstructure, chemical properties, and outgassing characteristics were analyzed. To ensure accurate comparison between different materials and coatings, the thermal history of all samples was carefully matched.

A. Sample preparation

ABS, PC and PP samples were fabricated using an open source Lulzbot Taz 6 fused filament fabrication (FFF) RepRap class 3-D printer (Aleph Objects, USA). The ABS filament was obtained from German RepRap GmbH (Feldkirchen, Germany), PC from Gizmo Dorks LLC (Temple City, California, USA) and PP from Ultimaker (Utrecht, The Netherlands). Sample dimensions were 30 mm × 30 mm × 1 mm. The printing parameters were set using open source Cura slicing software (21.08 Lulzbot edition), and the samples were printed with 100% infill with the parameters presented in Table 1. Both ABS and PP were printed directly onto the PEI surface of the print bed. In the case of PC, a thin layer of PVA-based glue was applied to the bed prior to printing to prevent the samples from adhering too tightly onto the print bed. After

printing, the glue was carefully removed from the PC samples with disposable laboratory wipes damped in water. Prior to further processing steps, all samples were cleaned by wiping them with cleanroom-compatible disposable wipes damped in water and isopropanol. The samples were handled with nitrile gloves at all stages of the experiments.

TABLE I. The printing parameters used to 3-D print the ABS, PC, and PP samples.

Plastic	**Layer height (mm)**	**Shell thickness (mm)**	**Bottom/top thickness (mm)**	**Print speed (mm/s)**	**Top/bottom speed (mm/s)**	**Print *T* (°C)**	**Bed *T* (°C)**	**Minimal layer time (s)**
ABS	0.15	1.0	0.8	60	60	245	95	15
PC	0.15	1.0	0.9	30	30	255	120	20
PP	0.18	1.0	1.08	50	10	235	60	15

The ABS, PC, and PP samples for the outgassing studies were prepared by coating the samples with either ALD AlO_x or Vacseal. The first sample set consisted of ALD-coated samples. AlO_x coatings were prepared with a Picosun R-100 top-flow ALD tool using trimethylaluminum ($Al(CH)_3$, TMA) and deionized water vapor as precursors and N_2 as carrier gas. The depositions were carried out at 80°C with a reactor pressure of 20 mTorr. The duration of the TMA pulse was 0.2 s, while the length of the water pulse was 0.5 s. The purging time between each precursor pulse was 5.0 s. In order to characterize the film growth, silicon wafers (Okmetic Oy, 100 mm, n-type, 512 µm, (100) orientation) were used as monitor samples. In an individual deposition, a single plastic sample was placed on top of a silicon wafer and coated with 300

cycles of TMA and water. All samples were coated in three similar consecutive runs, labeled runs I, II, and III, and a new silicon wafer was used in each run. The second sample set was fabricated by applying the Vacseal resin to the rest of the uncoated samples on all sides using an applicator brush, and by curing the resin at 95°C for 24 h. Additionally, the third sample set was made by applying Vacseal to the underside of some of the ALD coated samples and curing them with the aforementioned procedure. The vacuum and thermal histories of all sample sets were matched by pre-treatments detailed in [40]. This was done to ensure that the ALD-coated, resin-coated, and resin- and ALD-coated sample sets had outgassed and dehydrated similarly prior to testing.

B. Characterization

1. Thickness of deposited film

Thickness measurements were made on monitor wafers using a J. A. Woollam M2000UI ellipsometer. A thickness map was created for each monitor wafer, representing the thickness of alumina deposited on the 3-D printed plastic sample during that ALD run. Changes in the film uniformity are indirect indications of the modification of the outgassing properties or surface morphology of the plastic samples. For example, changes in thickness can be a subtle indicator of outgassing from the substrate during deposition. They can also indicate if there was a break in the deposition. Particulates with higher thickness than surrounding areas could be indicative of a more CVD nature to the deposition than ALD.

2. Microstructure and chemical analysis

To prepare samples for SEM imaging and EDS measurements, the ALD-coated samples were chilled to cryogenic temperatures in a liquid nitrogen bath, and subsequently bent until fracture. The fracture surface provided flat, un-altered views of the ALD coatings and subsurface of the samples.

Both backscatter (BSE) and secondary electron (SE) modes were implemented to image the ALD-coated sample fracture surfaces, and ALD layers. Imaging for the ABS and PC sample interiors (for porosity approximation) was done under a 15 kV accelerating voltage on a Hitachi S-4700 FE-SEM, while the PP sample and ALD layer imaging for all samples was done under 15 kV on a Philips XL40 ESEM.

Porosity fraction was calculated from SEM images processed in ImageJ[48]. The raw SEM images were thresholded to focus on pores in the image, and the surface area of those pores calculated in the program. Porous fractions in PC were determined from images at x10k magnification, whereas ABS porous fraction was approximated at x30k magnification, and PP at x2.5k. The difference in magnification used to calculate porous fraction was due to the difference in size and distribution of pores in each sample; the magnification was chosen to provide the most representative field of view possible.

A Transpector Inficon quadrupole residual gas analyzer (RGA), calibrated using 5.0 UHP nitrogen was used on the load lock of a modified Riber molecular beam epitaxy (MBE) system. The characterization chamber was equipped with a bespoke PID controlled nichrome wire heater capable of heating the sample from ambient temperature to 100°C. The sample was elevated using a SS 316 spacer such that the top of the sample was less than 10mm away from the RGA filament. The chamber was pumped down to 10^{-7} Torr using a turbo and a backing mechanical pump. After a 12-hour pump-down, each sample was heated in 10°C increments until the partial

pressures of outgassing entities saturated the RGA filament. This partial pressure data was collected using TWare32 gas analysis software. Further, this data was post-processed to normalize partial pressure of each molecular mass against a baseline collected with an empty chamber. The partial pressure of each molecular mass was normalized against the baseline during that run, which was then normalized against an empty chamber[40].

III. RESULTS AND DISCUSSION

First, the influence of the ABS, PC, and PP samples to the growth of the ALD films was considered. Film thickness maps measured with the ellipsometer for all monitor wafers are presented in Figure 1. In the case of a bare monitor wafer, the target film thickness was 50 nm per individual run. Based on the maps, it is clear that the presence of the plastic samples had a major impact on the thickness and uniformity of the AlO_x coating. For all samples after each deposition, there was an area of non-uniform growth on the wafer under the plastic samples, likely due to unintentional gas-phase chemical reactions between TMA and water vapor. For ABS samples, the thickness of the deposited film ranged from 18 to 58 nm for each sequential ALD run, and the uniformity of the films did not improve as reported[40]. For PC samples, the films became even less uniform with thickness ranging from 19 to 54 nm after deposition I and 30 to 88 nm after deposition III. In the case of PP samples, the film uniformity improved with each sequential deposition. However, the multicolored areas on the wafers underneath the samples are clear indications that the ALD process had not been optimal in the depositions.

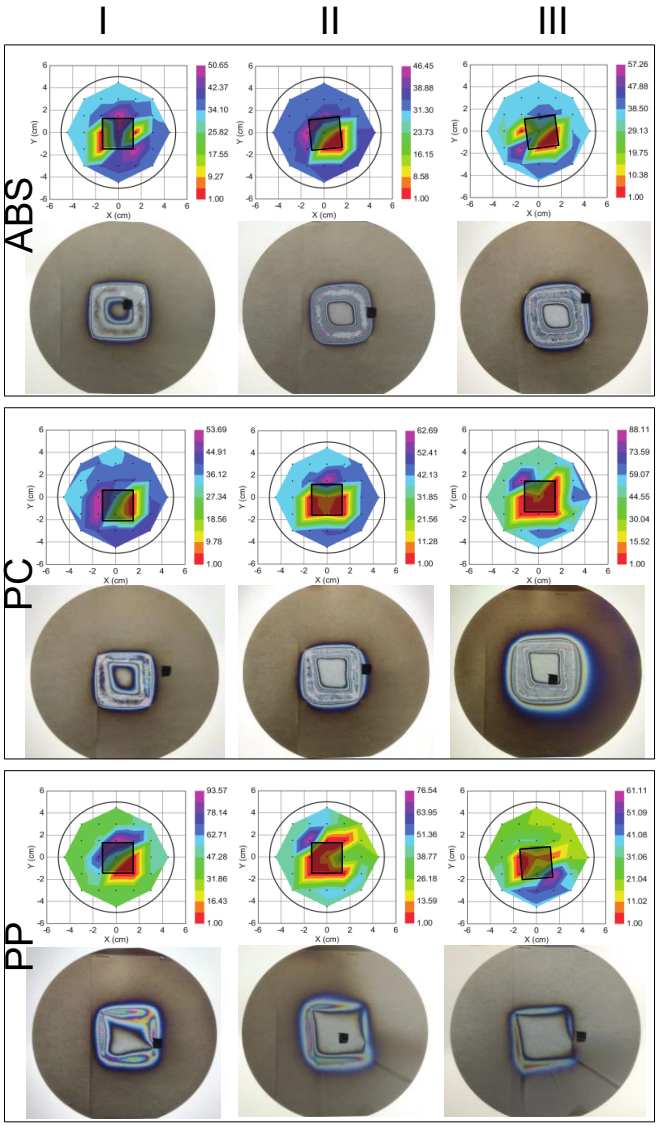

FIG 1. Ellipsometry maps showing thickness of AlO_x on sequential monitor wafers. The thickness scale (in nm) is represented as a color bar on the right of each map. The square in the middle of each map represents the location of the plastic sample. It is observed that the thickness around the middle, where the plastic sample was placed, is highly non-uniform and changes rapidly within a short distance. This non-uniform thickness was attributed to uncontrolled deposition in those areas that are partially covered by the plastic sample. In contrast, the thickness around the edges of the monitor wafers was found to be roughly constant. The targeted

thickness on silicon for each run was 50 nm but a deviation from this number was seen for each of the three sample types.

Macroscale porosity was seen in the case of as-printed PC. These evenly spaced pores were attributed to print trajectories[49]. The distance between the pores was measured to be constant at 320 μm while the pores at the widest were 250 μm (Figure 2). The presence of pores was indicative of insufficient flow of PC during the printing process. While there was no discernible difference in the quality of the PC parts as compared to ABS and PP, it was noted that for vacuum applications, PC should be printed at a slightly elevated temperature to fill up these pores[50-51]. The macropores were not seen post heat-treatment of samples.

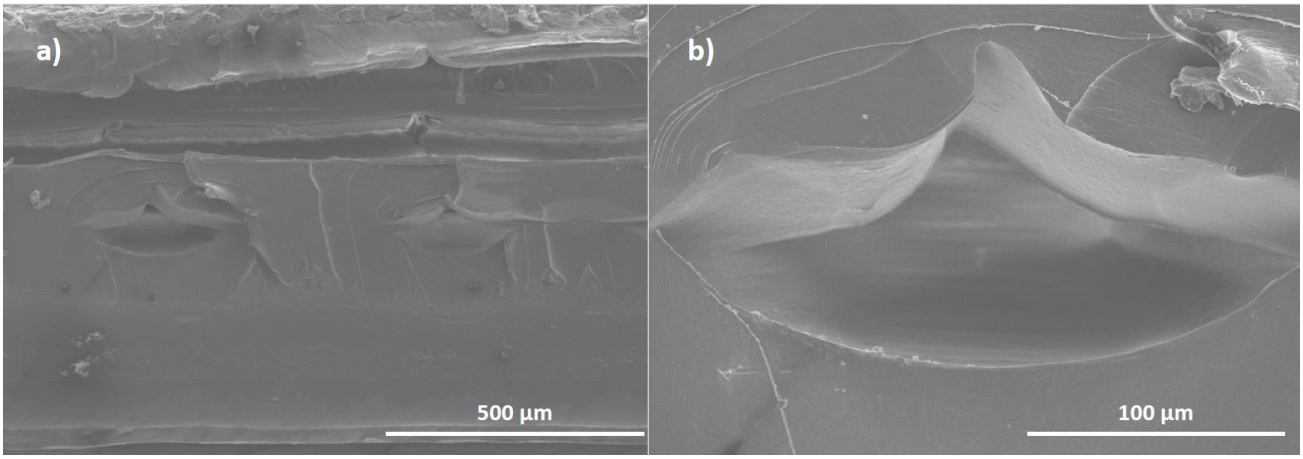

FIG 2. SEM image of macropores seen in PC. These are indicative of print lines.

Porous volume fraction (microscale porosity) of the 3-D printed polymer samples was found to be less than 10%, with PC approximated to be 0.1% porous, ABS 8% porous, and PP 2% porous. PC appeared to be devoid of porosity, whereas ABS contained circular pores of various sizes

(Figure 3). The PP sample exhibited a rough fracture surface, but did not exhibit many features that appeared to be pores. It should be noted that surface roughness on the fracture surfaces contributed to artifactual calculation of porosity for the PC and PP samples; however, the porosity determination method was kept consistent between the samples, leading to the calculation of some porosity in these samples. ALD coatings for the samples were observed to be thick and contiguous; an example of the film surface is provided for the PP sample in Figure 3d.

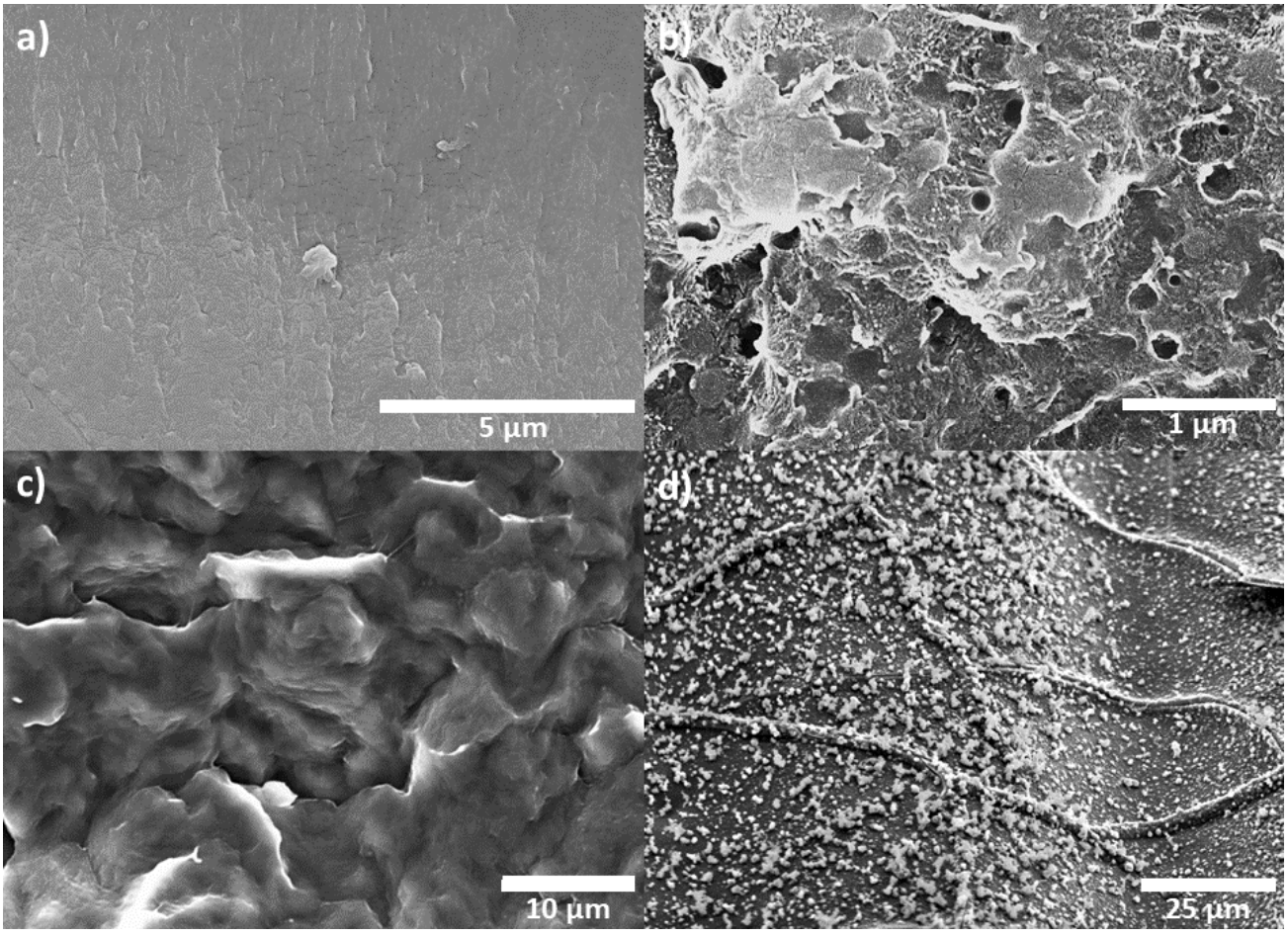

FIG 3. SE SEM cross section images of ALD-coated polymer samples: (a) PC (x10k), (b) ABS (x30k), and (c) PP (x2.5k); (d) shows the ALD coating on the surface of the PP sample

Apart from the underlying contiguous film, surface accumulation of AlO_x was seen in all samples. While in the case of PC, AlO_x particles were seen to form long rod-like structures, this behavior was not observed in ABS and PP. Surface particulates on ABS measured under 2 μm in length. In the case of PP, 3-D growth was observed with particles appearing to grow vertically in a fractal-like formation (Figure 4). Each of these particles was observed to be 1-2 μm in size with the entire stack measuring up to 5 μm. The presence of the surface particulate matter was attributed to the process not bring entirely in the ALD regime, degassing compounds, and high surface roughness of the underlying plastic. It was theorized that some of the TMA molecules may have desorbed from the polymer surface, leading to a reaction between TMA and water vapor taking place in the chamber and not on the surface of the sample. This formation of particulates could also be due to an incomplete purge cycle, which again results in the reaction taking place in the chamber and not on the surface of the sample. Since in a conventional ALD process gas phase reactions are not allowed, the process here was seen to happen at the cusp of the CVD and ALD regimes.

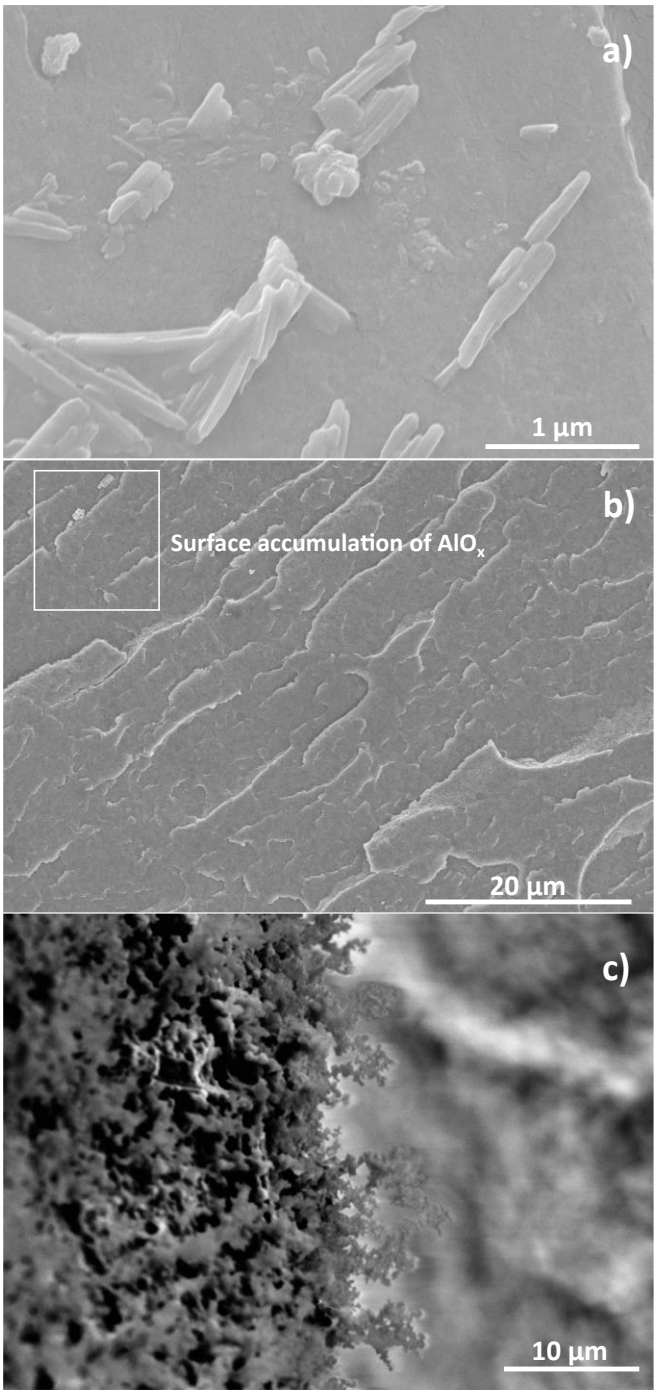

FIG 4. Surface accumulation of AlOx in the form of particles are seen in (a) PC (b) ABS and (c) PP.

The thickness of the ALD-deposited AlO_x layer on plastic was similar between clear PC and ABS, having thicknesses of 2.1 ± 0.3 μm and 2.3 ± 0.2 μm, respectively. The PP sample showed a substantially thinner layer, having a thickness of 0.88 ± 0.5 μm. The targeted thickness of AlO_x on the monitor wafer was 150 nm. Hence, the much higher apparent thickness on plastic samples speaks to the porosity of samples and the much higher diffusion of TMA and water vapor through the plastic.

It appears that the absence of subsurface porosity results in no subsurface crystallites, such as was observed in the PC and PP samples (Figure 5). Where subsurface porosity was present, as in the ABS sample, there were crystallites below the polymer sample surface.

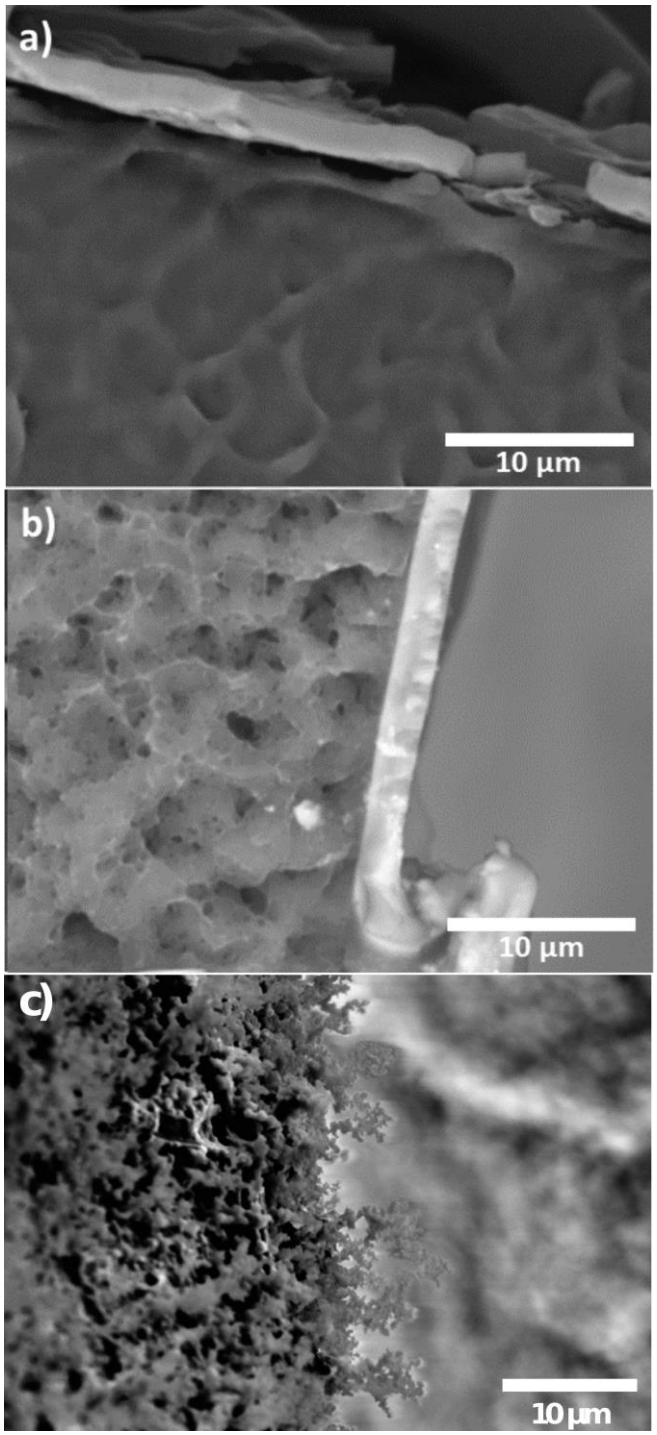

FIG 5. BSE SEM cross section images of ALD-coated polymer samples: (a) PC, (b) ABS and (c) PP. Note that all images are at magnification of x3.5k.

To measure the penetration depth of the TMA into the 3-D printed polymer surfaces, EDS line scans measuring Al Kα signal were taken on cross sections of the ALD-coated samples perpendicular to the surface (see Figure 5 for field of view for these line scans). The differences in porosity, presence of subsurface crystallites, and density of each individual polymer likely impacted the sampling volume and Al Kα signal intensity for each of EDS line scans. It should be noted that the EDS line scan data presented is located with the 0 μm depth at the oxide/polymer interface.

The difference in TMA diffusion depth was found to be both a function of polymer composition, glass transition temperature, porosity, and characteristics of the ALD-forming film. Looking at the Al Kα profiles for the clear polymer samples (Figure 6), clear ABS showed the least penetration, with clear PP having a somewhat higher penetration, and clear PC having a very deep Al Kα profile.

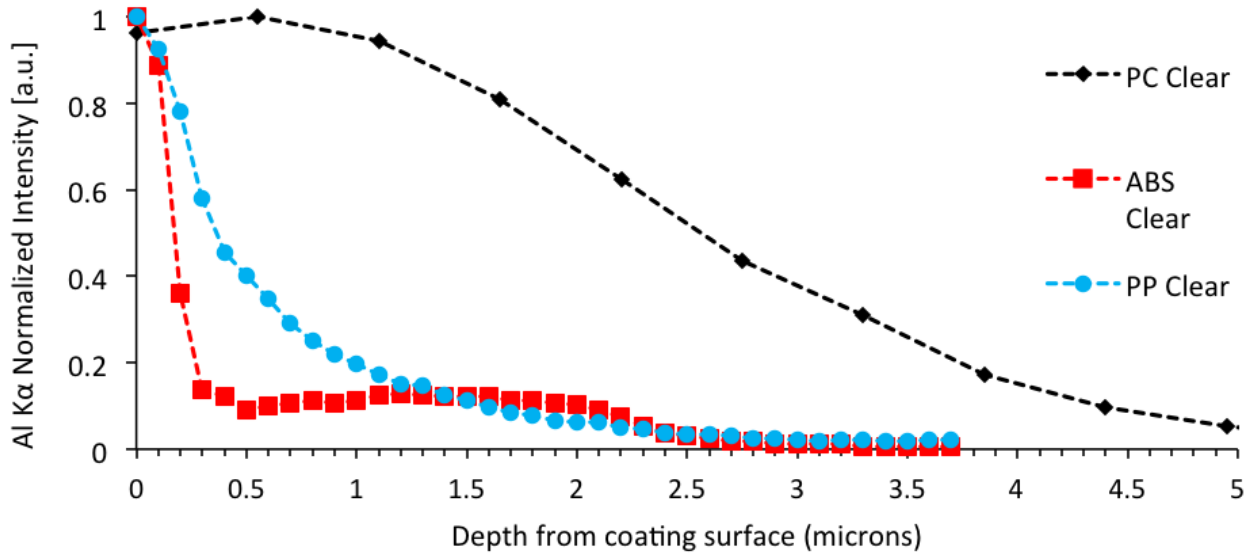

FIG 6. EDS depth profiles for Al Kα for ALD-coated 3-D printed polymer samples

The sum of normalized partial pressures as a function of temperature for all polymers and atomic masses 1 to 100 is shown in Figure 7. For all plastics considered, the ALD coated samples registered consistently lower outgassing. Also, it was noted that all ALD coated samples could be successfully heated to 100°C without reaching RGA maximum pressure limits. Additionally, the Vacseal resin coated ABS sample could be heated to 100°C. The trend was that all Vacseal coated samples could only be heated up to 60°C - 70°C. Generally, the outgassing increased with increasing temperature. While in case of ABS the ALD + Vacseal resin coated sample registered higher outgassing than the sample coated with just Vacseal, it is difficult to draw similar conclusions about the PC and PP samples.

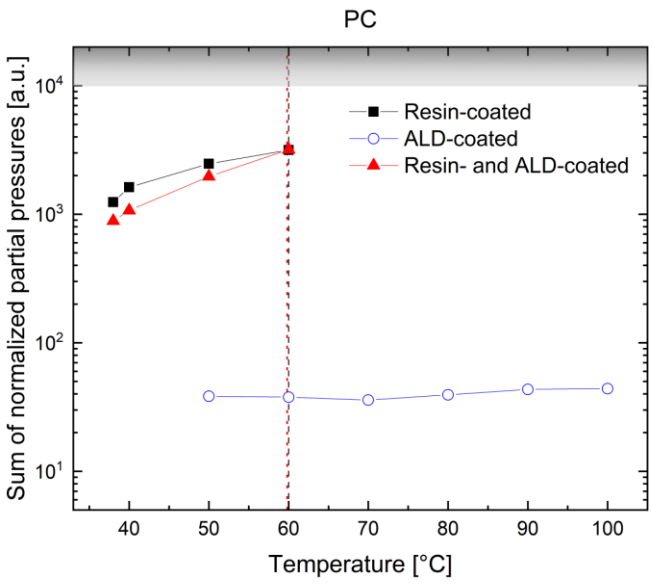
PC
Sum of normalized partial pressures [a.u.]
Temperature [°C]
Resin-coated
ALD-coated
Resin- and ALD-coated

(a)

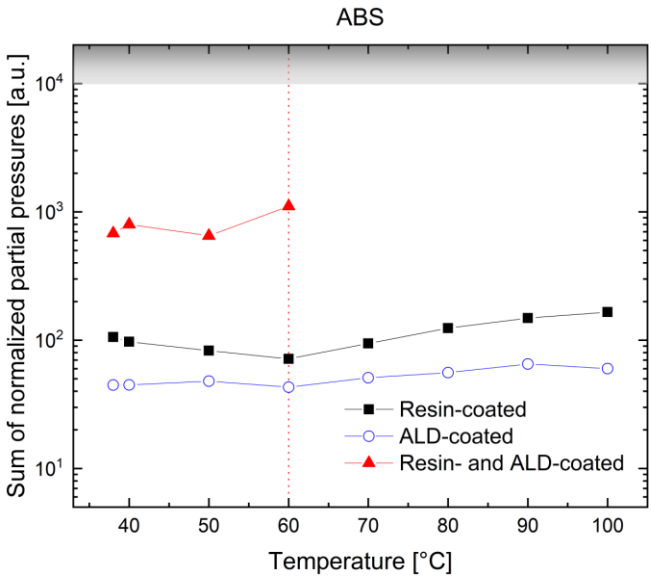
ABS
Sum of normalized partial pressures [a.u.]
Temperature [°C]
Resin-coated
ALD-coated
Resin- and ALD-coated

(b)

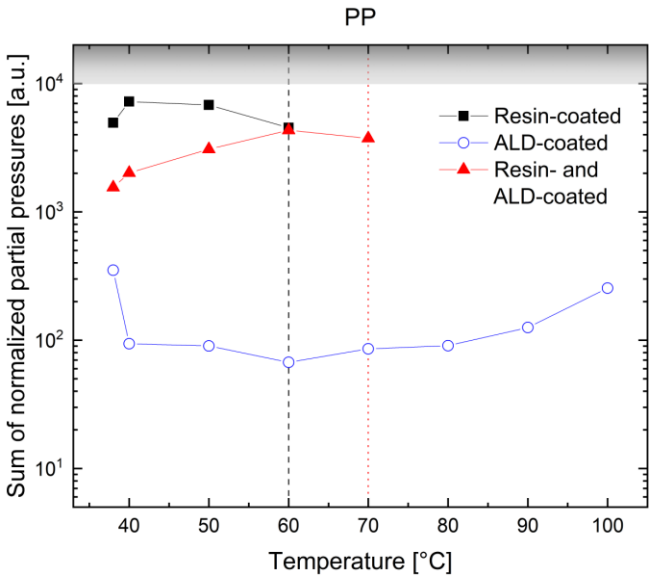
PP
Sum of normalized partial pressures [a.u.]
Temperature [°C]
Resin-coated
ALD-coated
Resin- and
ALD-coated

(c)

FIG 7. Sum of normalized partial pressures at all measured temperatures for (a) PC, (b) ABS, (c) PP. The vertical dashed lines indicate temperature setpoints after which partial pressure could not be measured without damaging equipment. The grey area represents a region of high outgassing where data collection is not possible with the RGA used in this study.

All sample data, ALD coated, resin-coated, and resin- and ALD-coated, could be gathered for temperatures up to 60°C. After 60°C some of these samples registered high degrees of outgassing and the RGA could not be safely operated. Hence all comparison is done at 60°C. A comparison using the methodology employed in [40] is shown in Figure 8. In addition, Figure 9 represents partial pressures (Torr) of all molecular masses 1 to 100 with the baseline subtracted out. The scale has been kept consistent to compare absolute pressures. Also, a table of sum of partial pressures at different temperatures in included in the supplementary material.

Compared to ALD-coated samples, the resin-coated samples registered higher relative outgassing. This is due to incomplete curing of the resin[40]. The application of Vacseal to the samples is a manual process using the brush provided by the manufacturer. Often a layer that is too thick may be deposited. When this layer is cured at room temperature it can take several weeks[52]. The high outgassing seen from the Vacseal coated sample is attributed to the solvents present in Vacseal. The peak at 91 AMU was matched to xylene, ethylbenzene and toluene – the main components of Vacseal[53-54]. Without an effective curing method, Vacseal is not recommended as a sealant for plastics used in vacuum applications. Effective curing of Vacseal happens at elevated temperatures, which most polymeric materials cannot tolerate.

The partial pressures of outgassed entities from ALD coated samples were consistently lower for all materials, making an ALD coating, despite its non-uniformity, the best choice to inoculate polymers against outgassing. It should be noted that no data could be collected for uncoated

polymers because their outgassing was too great for the equipment used and the Vacseal coating reduced outgassing enough to enable sample pump down to 10^{-7} Torr.

The relative outgassing characteristics of ALD coated PC, ABS and PP were very similar, with PC and ABS registering sharp drops at certain atomic numbers. In comparison, the outgassing seen in case of ALD coated PP was more stable.

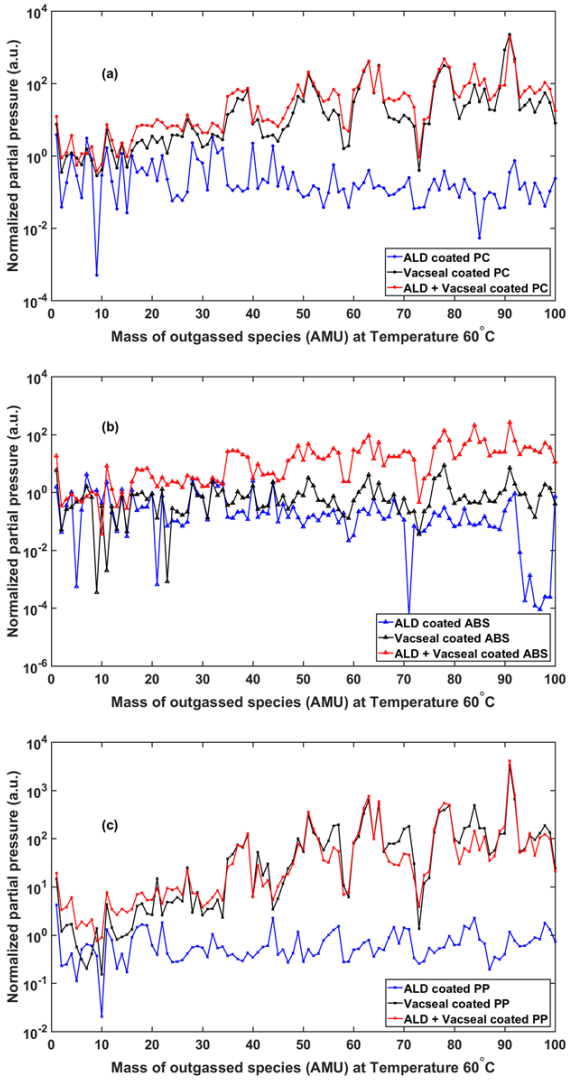

FIG 8. Outgassing characteristics of clear PC (a), ABS (b) and PP (c) at molecular masses 1 to 100 at 60°. A consistently low value of normalized partial pressure was seen for all ALD coated samples.

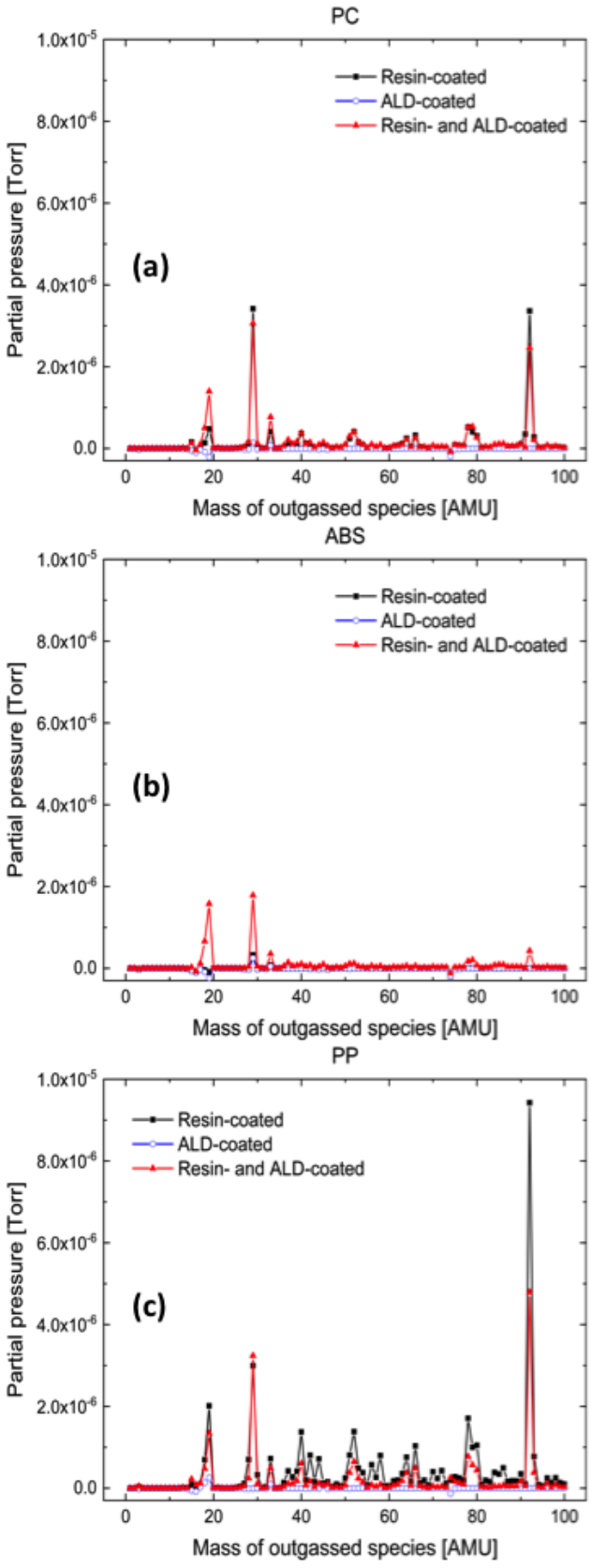
PC
Resin-coated
ALD-coated
Resin- and ALD-coated
(a)
Partial pressure [Torr]
Mass of outgassed species [AMU]
ABS
(b)
PP
(c)

FIG 9. Outgassing characteristics of clear PC (a), ABS (b) and PP (c) at molecular masses 1 to 100 at 60° with background subtraction. A consistently low value of normalized partial pressure was seen for all ALD coated samples.

The porosity of the 3-D printed materials can make the use of ABS, PC, and PP challenging for vacuum applications, as increased surface area and relatively large pores have the potential to trap atmospheric gases into the materials. Especially in the case of PC, the extent of macroscale porosity can likely be reduced by increasing the flow rate of the filament, using a higher nozzle temperature, and optimizing the print speed in the printing process. Similar optimization can yield a smaller extent of pores and surface roughness for ABS and PP, as well. Another factor than can influence the formation of pores during the printing is the moisture content of the plastics, which can be reduced by pre-baking the filaments at an elevated temperature prior to the printing, and enclosing the filaments in a desiccant chamber during the printing process. Additionally, the surfaces of 3-D printed components intended for vacuum applications can possibly be smoothened by mechanical polishing or solvent vapor treatments prior to coating them with ALD materials or resins.

The ALD process employed in these studies was not optimal for the highly porous 3-D printed plastics. Longer purge steps between the precursor pulses are expected to yield more uniform film coverage on the 3-D printed plastics samples. This, in turn, could improve the outgassing characteristics of the plastics even further, as pinhole-free ALD AlO_x films are efficient gas barriers[28-29]. The length of the precursor pulses could as well be tuned to ensure sufficient coverage of the plastic surface with the AlO_x film. In addition, the plastic sample could be heat

treated before the ALD deposition to minimize outgassing in the reactor chamber and allow a more uniform, higher quality deposition.

While most ALD films observed were continuous, there were certain defects observed, such as, the break in the coating seen in Figure 5 (a). Despite these defects the coatings were deemed to be effective outgassing barriers at the measured pressures. In order to reduce outgassing further, which may be necessary for certain contamination-sensitive applications[55-59], it would be useful to characterize the outgassed species, its effect on the tooling and other samples processed either in the same or subsequent runs. Further research is also recommended to study the mechanism behind outgassing reduction when ALD films are used as barrier coatings. In addition, 3-D printing parameters have an impact on porosity and surface finish, which in turn affect how contiguous the barrier coating will be. Several other factors, such as, a specific polymer's affinity towards a certain precursor molecule needs to be studied too[47,60]. The main limitation of the outgassing data shown in this study is that it was collected after 12 hours of pump down, when the system was under very high vacuum. It is reported that some species, such as water vapor, selectively outgas in the mTorr pressure range[61-62]. Hence, a kinetic study of partial pressure measurement, while the system is pumping down is recommended.

When these 3-D printed plastics are sealed effectively, they could be used in vacuum environments as substrates, replacement parts and as whole systems.

IV. CONCLUSIONS

Unpigmented 3-D printed PC, ABS and PP were coated with two types of barrier coatings, an ALD AlO_x layer and a commercially available resin Vacseal, in order to study their vacuum compatibility. The low levels of porosity seen in these polymers coupled with the absence of a

potentially volatile pigment made them suitable candidates to be tested for outgassing in a vacuum environment. In both cases, a reduction in relative outgassing was observed as compared to uncoated films under a very high vacuum. Further, the ALD coated samples registered lower pressures than the resin coated ones, showing an ALD film to be effective at inoculating plastics in a vacuum environment.

ACKNOWLEDGMENTS

This work was partially supported by Fulbright Finland, the Witte endowment and Aleph Objects. The authors acknowledge the provision of facilities by Aalto University at OtaNano – Micronova Nanofabrication Centre and at the RawMatTERS (RAMI) facilities, and the Applied Chemical and Morphological Analysis Laboratory at Michigan Tech for use of the instruments and staff assistance. I.T.S.H. acknowledges the financial support from AaltoELEC Doctoral School and Walter Ahlström foundation. G.M. and M.K. gratefully acknowledge funding from the Strategic Research Council at the Academy of Finland (CloseLoopConsortium, Grant No. 303452).

References

1 K. Wong and A. Hernandez, ISRN Mechanical Engineering 2012, (2012).

2 D. Schniederjans, International Journal of Production Economics 183, (2017).

3 N. Guo and M. Leu, Frontiers of Mechanical Engineering 8, (2013).

4 B. Wittbrodt, A. Glover, J. Laureto, G. Anzalone, D. Oppliger, J. Irwin and J. Pearce, Mechatronics 23, (2013).

5 A. Laplume, B. Petersen and J. Pearce, Journal of International Business Studies 47, (2016).

6 J. Pearce, Science 337, (2012).

7 J. Pearce, *Open-source lab: how to build your own hardware and reduce research costs*, (2013).

8 T. Baden, A. Chagas, G. Gage, T. Marzullo, L. Prieto-Godino and T. Euler, PLOS Biology 13, (2015).

9 M. Coakley and D. Hurt, Journal Of Laboratory Automation 21, (2016).

10 I. Petrick and T. Simpson, Research-Technology Management 56, (2013).

11 B. Berman, Business Horizons 55, (2012).

12 D. Bak, Assembly Automation 23, (2003).

13 J. Pearce, Science and Public Policy 43, (2015).

14 T. Pasanen, G. von Gastrow, I. Heikkinen, V. Vähänissi, H. Savin and J. Pearce, Materials Science in Semiconductor Processing 89, (2019).

15 I. Hietanen, I. Heikkinen, H. Savin and J. Pearce, Hardwarex 4, (2018).

16 J. Dever, S. Miller, E. Sechkar and T. Wittberg, High Performance Polymers 20, (2008).

17 Hall, D. and Fote, A., *26th Thermophysics Conference*, (1991).

18 J. Townsend, P. Hansen, J. Dever, K. de Groh, B. Banks, L. Wang and C. He, High Performance Polymers 11, (1999).

19 T. Zuby, K. Degroh and D. Smith, *Degradation of FEP Thermal Control Materials Returned From The Hubble Space Telescope (No. N--96-18436; NASA-TM--104627; NAS--1.15: 104627; REPT--96B00024; NIPS--96-07908).* (National Aeronautics and Space Administration, Greenbelt, MD (United States). Goddard Space Flight Center., 1995).

20 J. Dever, K. de Groh, B. Banks and J. Townsend, High Performance Polymers 11, (1999).

21 W. Campbell Jr, R. Marriott and J. Park, *Outgassing Data for Selecting Spacecraft Materials* (National Aeronautics and Space Administration, 1984).

22 J. Gaier, M. Brinkmeier and E. Gaier, in (NASA CONFERENCE PUBLICATION, 2020), pp. 257-268.

23 R. Elsey, Vacuum 25, (1975), pp. 299-306.

24 J. Kwon, H. Jung, I. Yeo and T. Song, Vacuum 85, (2011).

25 R. Elsey, Vacuum 25, (1975), pp. 347-361.

26 W. Perkins, Journal of Vacuum Science and Technology 10, (1973).

27 A.J. Muller, L.A. Psota-Kelty, H.W. Krautter and J.D. Sinclair, Solid State Technology 37, (1994).

28 T. Hirvikorpi, M. Vähä-Nissi, A. Harlin, J. Marles, V. Miikkulainen and M. Karppinen, Applied Surface Science 257, (2010).

29 T. Hirvikorpi, M. Vähä-Nissi, A. Harlin and M. Karppinen, Thin Solid Films 518, (2010).

30 J. Lange and Y. Wyser, Packaging Technology and Science 16, (2003).

31 H. Chatham, Surface And Coatings Technology 78, (1996).

32 S. Park, J. Oh, C. Hwang, J. Lee, Y. Yang and H. Chu, Electrochemical and Solid-State Letters 8, (2005).

33 A. Ghosh, L. Gerenser, C. Jarman and J. Fornalik, Applied Physics Letters 86, (2005).

34 J. Meyer, D. Schneidenbach, T. Winkler, S. Hamwi, T. Weimann, P. Hinze, S. Ammermann, H. Johannes, T. Riedl and W. Kowalsky, Applied Physics Letters 94, (2009).

35 T. Minton, B. Wu, J. Zhang, N. Lindholm, A. Abdulagatov, J. O'Patchen, S. George and M. Groner, ACS Applied Materials & Interfaces 2, (2010).

36 G. Pluvinage, Springer Science & Business Media, (2003).

37 E. Kelly, The Journal Of Prosthetic Dentistry 21, (1969).

38 D. Rickerby and N. MacMillan, Wear 60, (1980).

39 Vacseal.Net (2020).

40 I. Heikkinen, G. Marin, N. Bihari, C. Ekstrum, P. Mayville, Y. Fei, Y. Hu, M. Karppinen, H. Savin and J. Pearce, Surface and Coatings Technology 386, (2020).

41 B. Puri and R. Bansal, Carbon 1, (1964).

42 N. Tanikella, B. Wittbrodt and J. Pearce, Additive Manufacturing 15, (2017).

43 A. Davis and J. Golden, Journal Of Macromolecular Science, Part C 3, (1969).

44 J. Cantrell, S. Rohde, D. Damiani, R. Gurnani, L. DiSandro, J. Anton, A. Young, A. Jerez, D. Steinbach, C. Kroese and P. Ifju, Rapid Prototyping Journal 23, (2017).

45 W. Zhu, S. Pyo, P. Wang, S. You, C. Yu, J. Alido, J. Liu, Y. Leong and S. Chen, ACS Applied Materials & Interfaces 10, (2018).

46 I. Heikkinen, C. Kauppinen, Z. Liu, S. Asikainen, S. Spoljaric, J. Seppälä, H. Savin and J. Pearce, Additive Manufacturing 23, (2018).

47 Outgassing.Nasa.Gov (2020).

48 Imagej.Nih.Gov (2020).

49 S. Guessasma, S. Belhabib and H. Nouri, Polymers 11, (2019).

50 Y. Song, Y. Li, W. Song, K. Yee, K. Lee and V. Tagarielli, Materials & Design 123, (2017).

51 I. Gajdoš and J. Slota, Tehnički Vjesnik 20, (2013).

52 Application Notes on Vacseal, 2Spi.Com (2020).

53 Vacseal SDS, Vacseal.Net (2020).

54 Webbook.Nist.Gov (2020).

55 T. Patrick, Vacuum 23, (1973).

56 K. Fayazbakhsh and A. Abedian, Advances In Space Research 45, (2010).

57 A. Neuber, M. Butcher, H. Krompholz, L. Hatfield and M. Kristiansen, IEEE Transactions On Plasma Science 28, (2000).

58 N. Ridley and Z. Wang, Materials Science Forum 233-234, (1996).

59 D. Storm, T. McConkie, M. Hardy, D. Katzer, N. Nepal, D. Meyer and D. Smith, Journal Of Vacuum Science & Technology B, Nanotechnology And Microelectronics: Materials, Processing, Measurement, And Phenomena 35, (2017).

60 M. Sefa, Z. Ahmed, J. Fedchak, J. Scherschligt and N. Klimov, Journal Of Vacuum Science & Technology A: Vacuum, Surfaces, And Films 34, (2016).

61 R. Grinham and A. Chew, Applied Science And Convergence Technology 26, (2017).

62 G.P. Beukema, Cursus Vacuumtechnologie (2016).

ABS

PC

PP

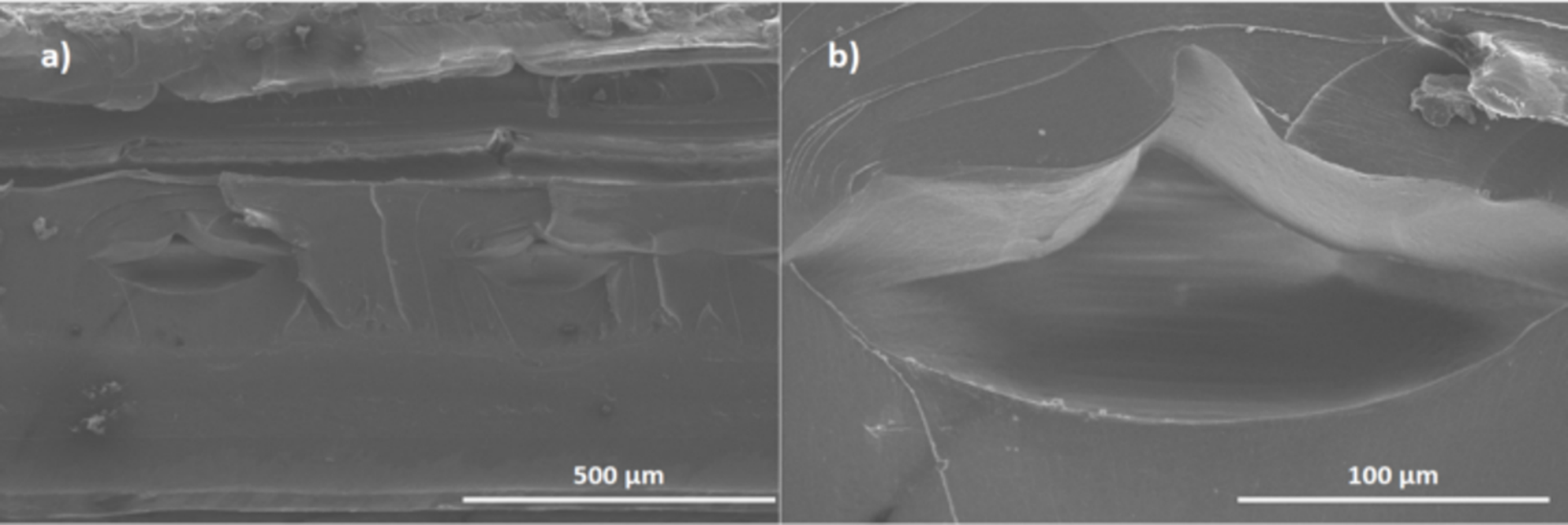
a)
500 µm
b)
100 µm

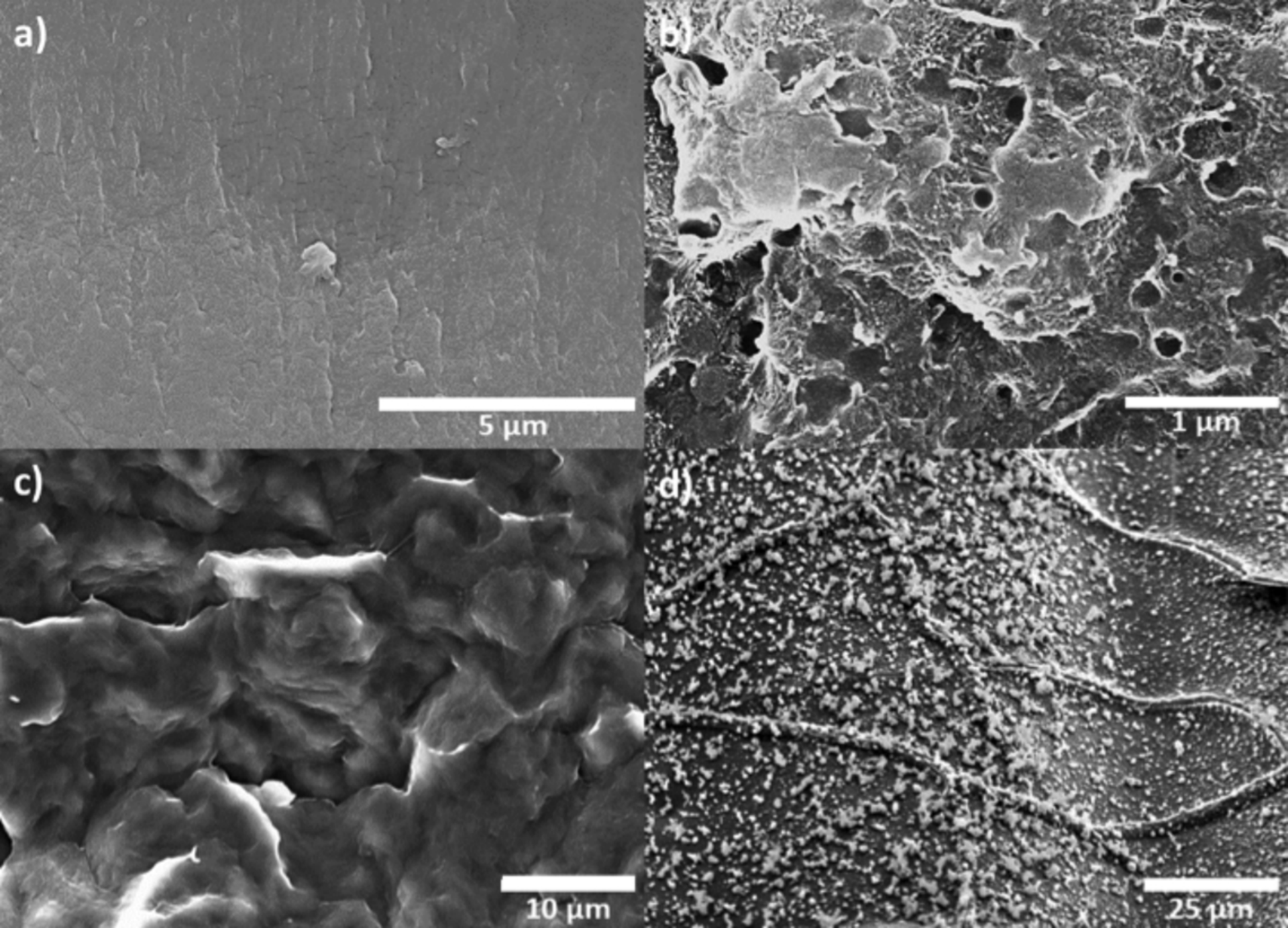
a)
5 µm
b)
1 µm
c)
10 µm
d)
25 µm

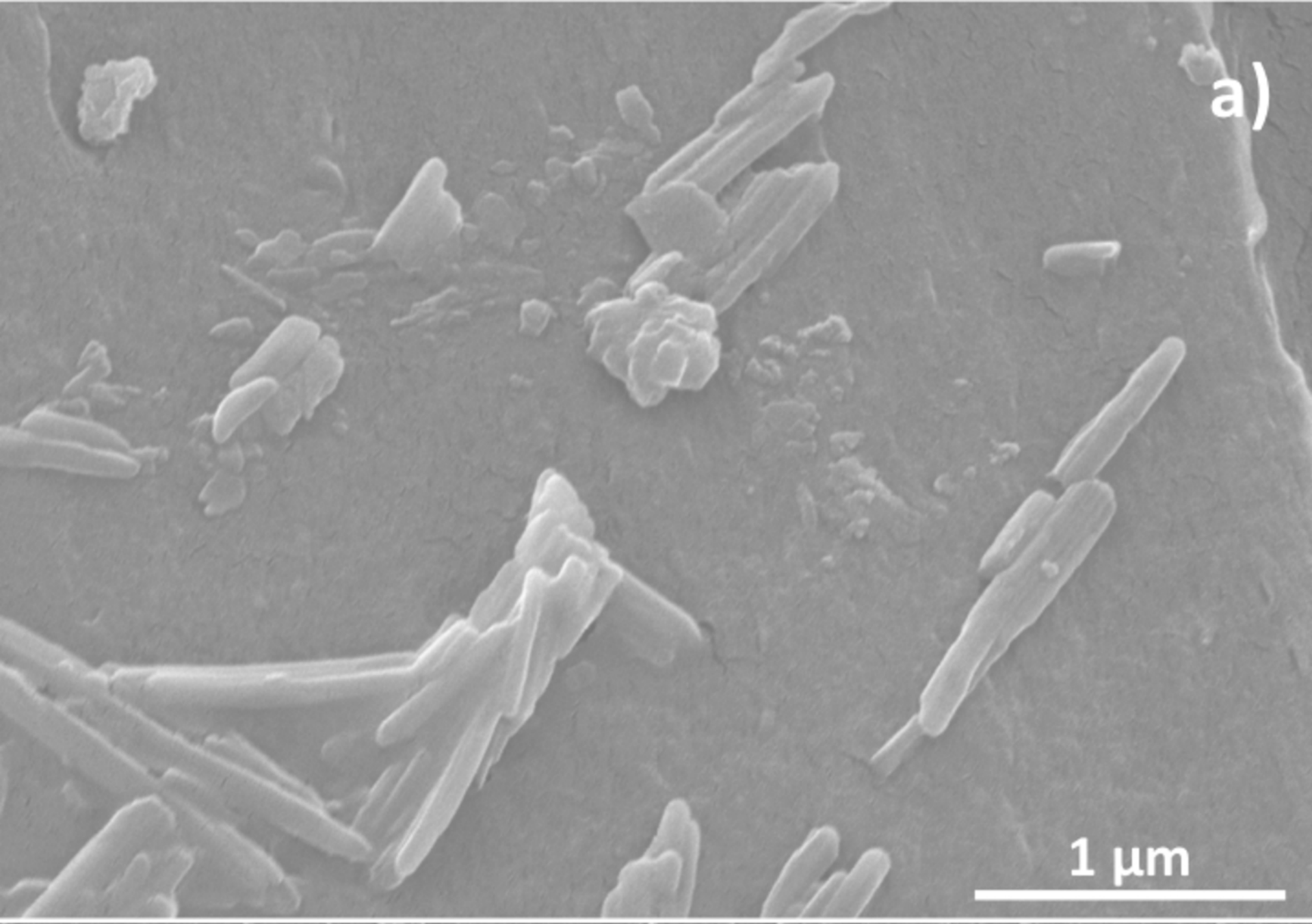
a)
1 µm

b)
Surface accumulation of AlO_x
20 µm

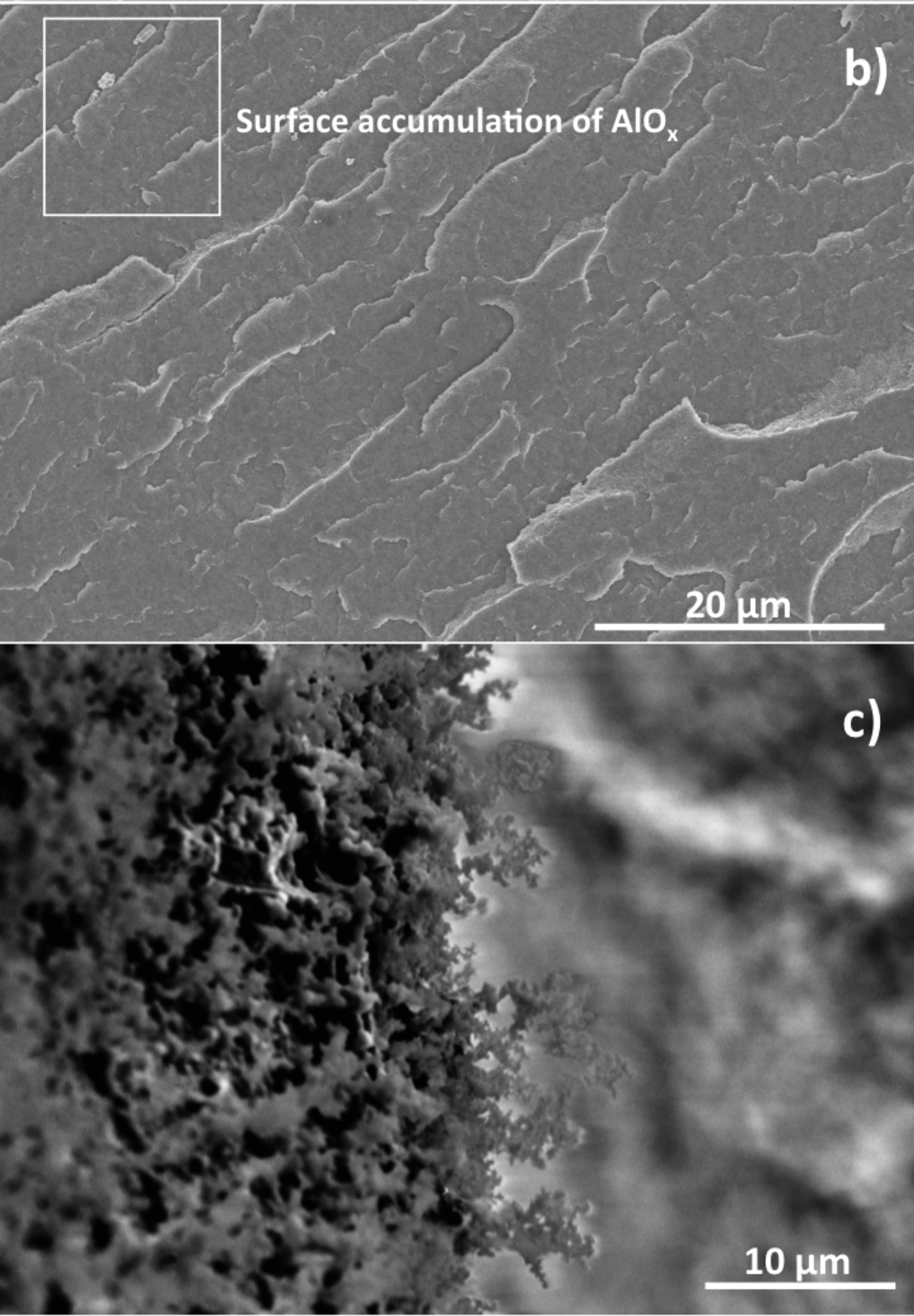
c)
10 µm

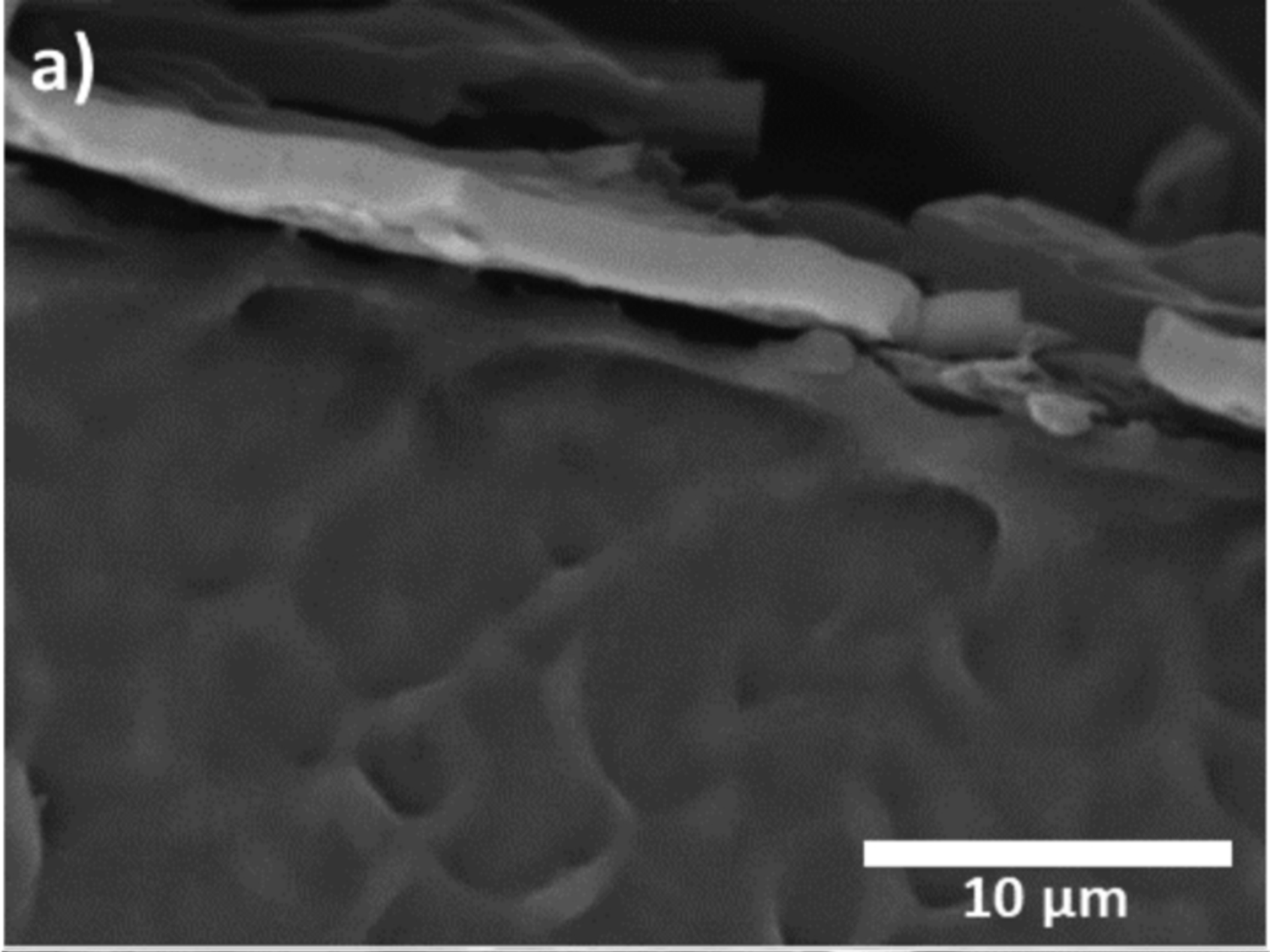
a)
10 µm

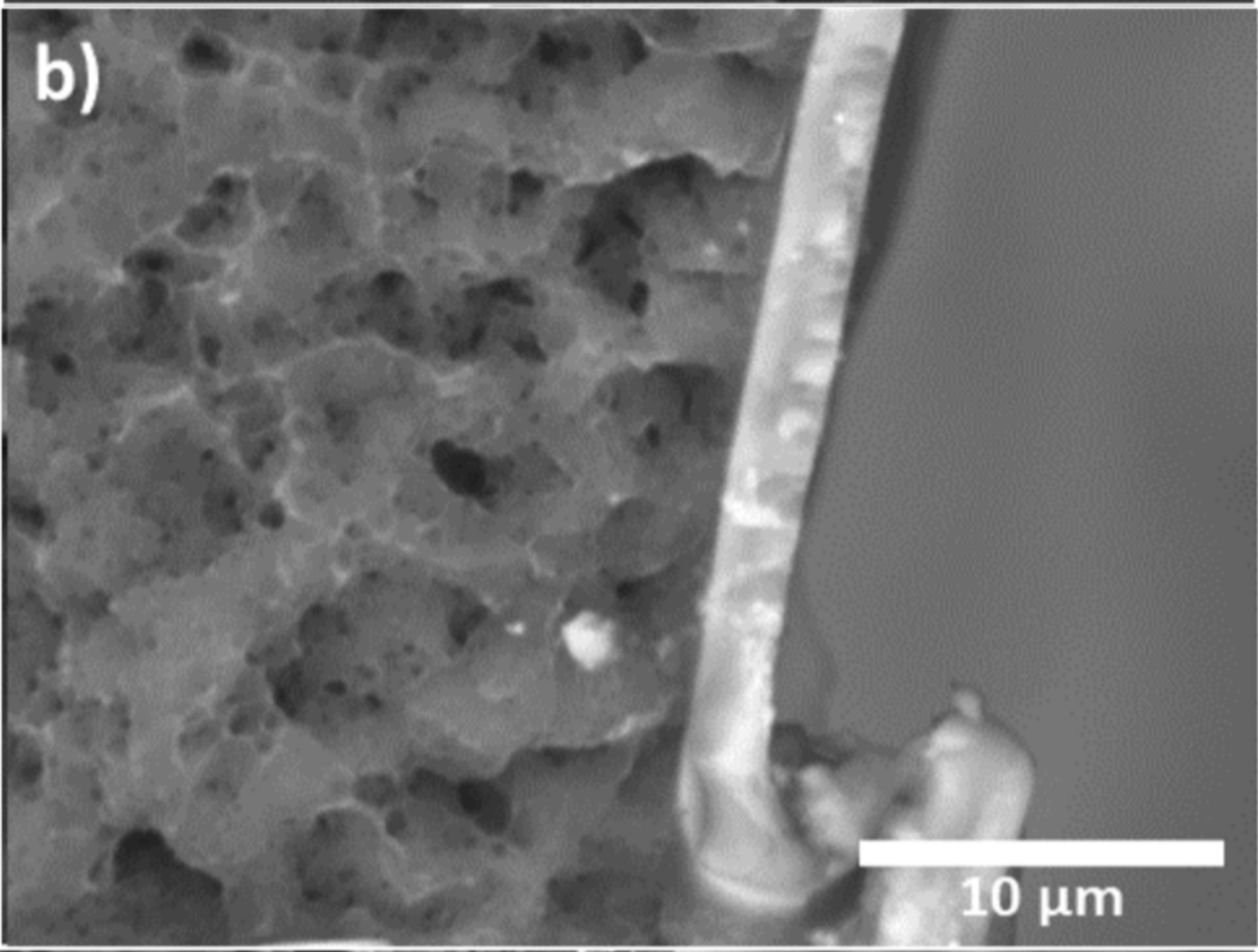
b)
10 µm

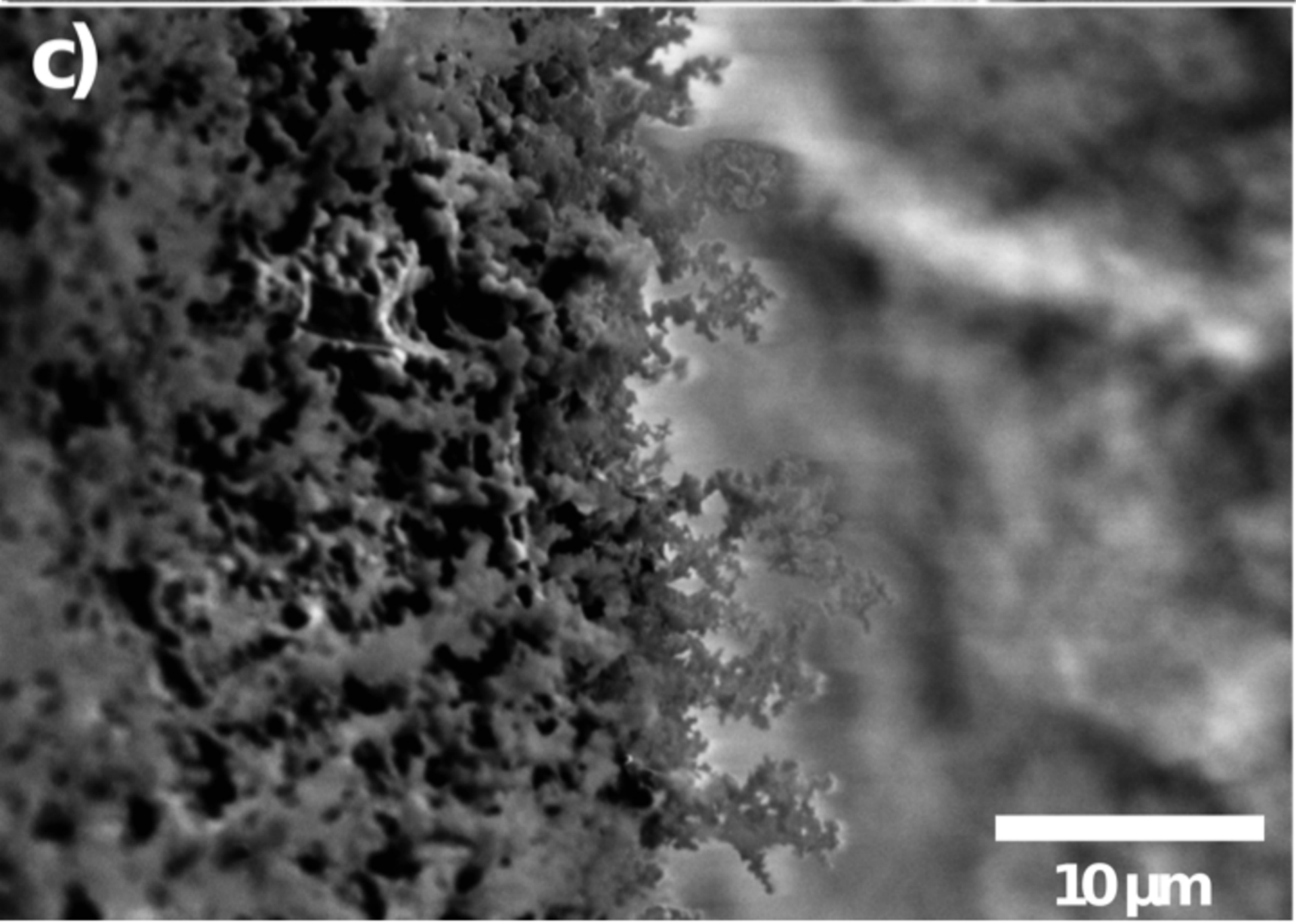
c)
10 µm

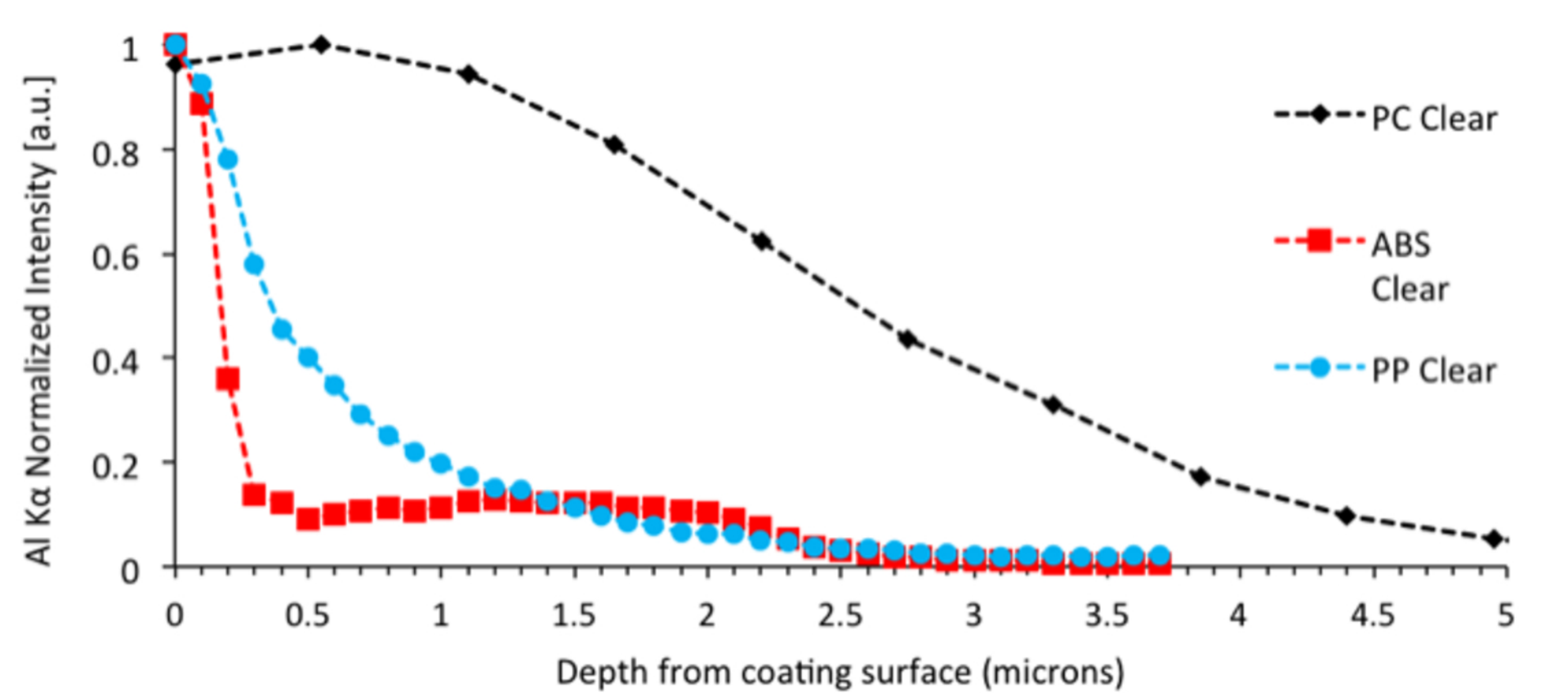
Al Kα Normalized Intensity [a.u.]
1
0.8
0.6
0.4
0.2
0
0
0.5
1
1.5
2
2.5
3
3.5
4
4.5
5
Depth from coating surface (microns)
PC Clear
ABS Clear
PP Clear

PC

Sum of normalized partial pressures [a.u.]

10^4
10^3
10^2
10^1

Resin-coated
ALD-coated
Resin- and ALD-coated

40 50 60 70 80 90 100

Temperature [°C]

(a)

ABS

Sum of normalized partial pressures [a.u.]

10^4
10^3
10^2
10^1

Resin-coated
ALD-coated
Resin- and ALD-coated

40 50 60 70 80 90 100

Temperature [°C]

(b)

PP

Sum of normalized partial pressures [a.u.]

10^4
10^3
10^2
10^1

Resin-coated
ALD-coated
Resin- and ALD-coated

40 50 60 70 80 90 100

Temperature [°C]

(c)

(a)

Normalized partial pressure (a.u.)

10^{4} 10^{2} 10^{0} 10^{-2} 10^{-4}

0 10 20 30 40 50 60 70 80 90 100

Mass of outgassed species (AMU) at Temperature 60°C

ALD coated PC
Vacseal coated PC
ALD + Vacseal coated PC

(b)

Normalized partial pressure (a.u.)

10^{4} 10^{2} 10^{0} 10^{-2} 10^{-4} 10^{-6}

0 10 20 30 40 50 60 70 80 90 100

Mass of outgassed species (AMU) at Temperature 60°C

ALD coated ABS
Vacseal coated ABS
ALD + Vacseal coated ABS

(c)

Normalized partial pressure (a.u.)

10^{4} 10^{3} 10^{2} 10^{1} 10^{0} 10^{-1} 10^{-2}

0 10 20 30 40 50 60 70 80 90 100

Mass of outgassed species (AMU) at Temperature 60°C

ALD coated PP
Vacseal coated PP
ALD + Vacseal coated PP

PC

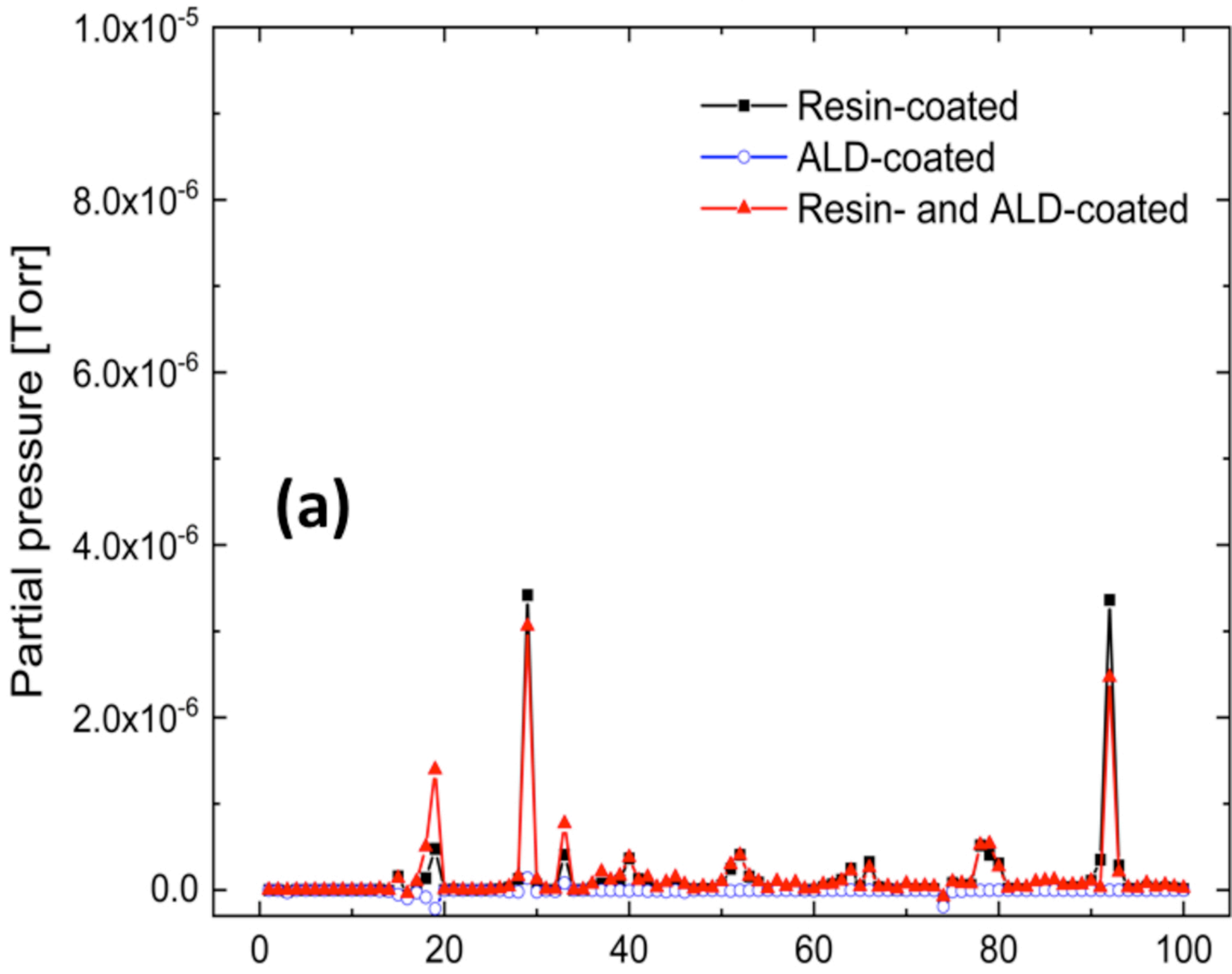
Resin-coated
ALD-coated
Resin- and ALD-coated
(a)
Partial pressure [Torr]
1.0x10-5
8.0x10-6
6.0x10-6
4.0x10-6
2.0x10-6
0.0
0
20
40
60
80
100
Mass of outgassed species [AMU]

ABS

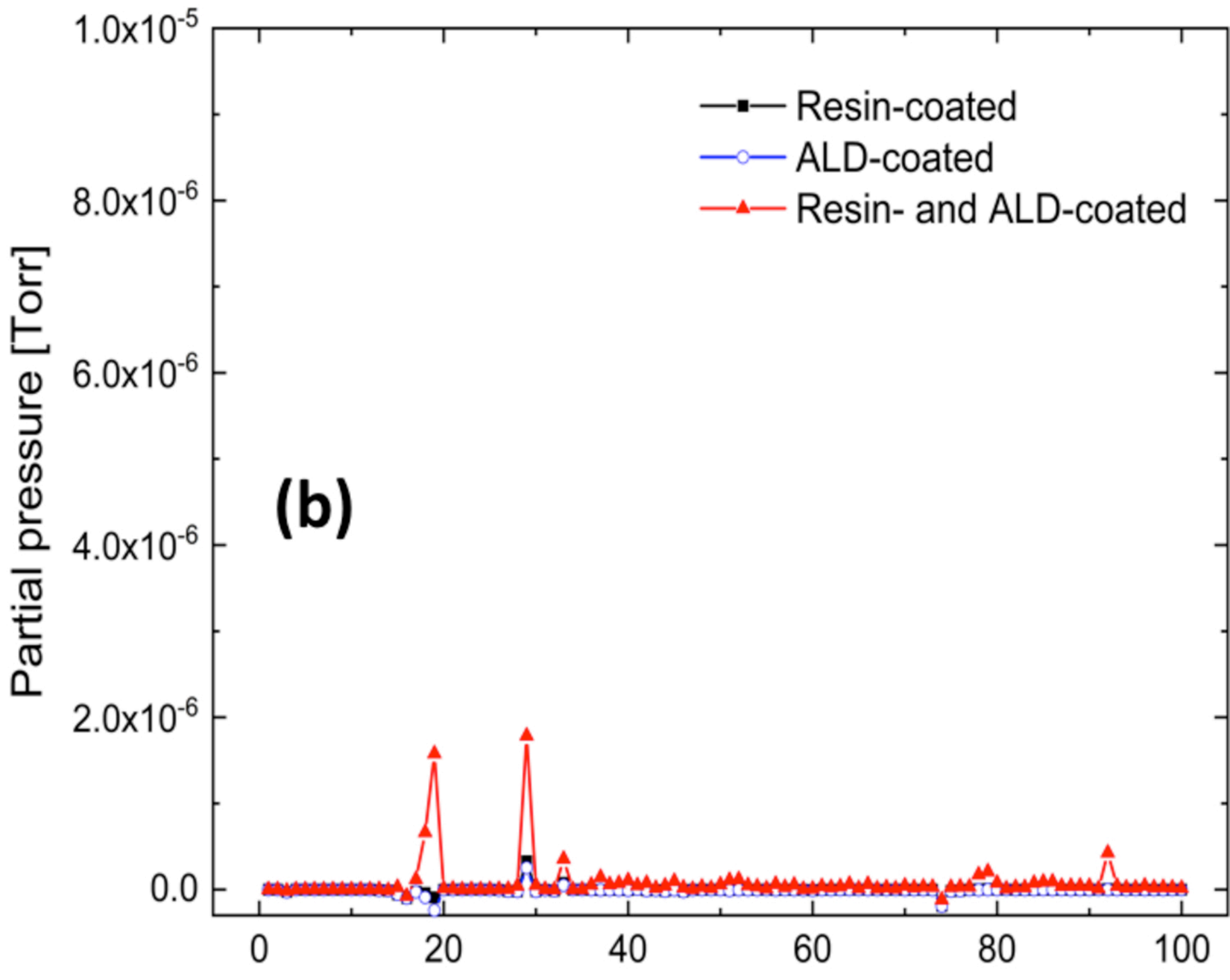
Resin-coated
ALD-coated
Resin- and ALD-coated
(b)
Partial pressure [Torr]
1.0x10-5
8.0x10-6
6.0x10-6
4.0x10-6
2.0x10-6
0.0
0
20
40
60
80
100
Mass of outgassed species [AMU]

PP

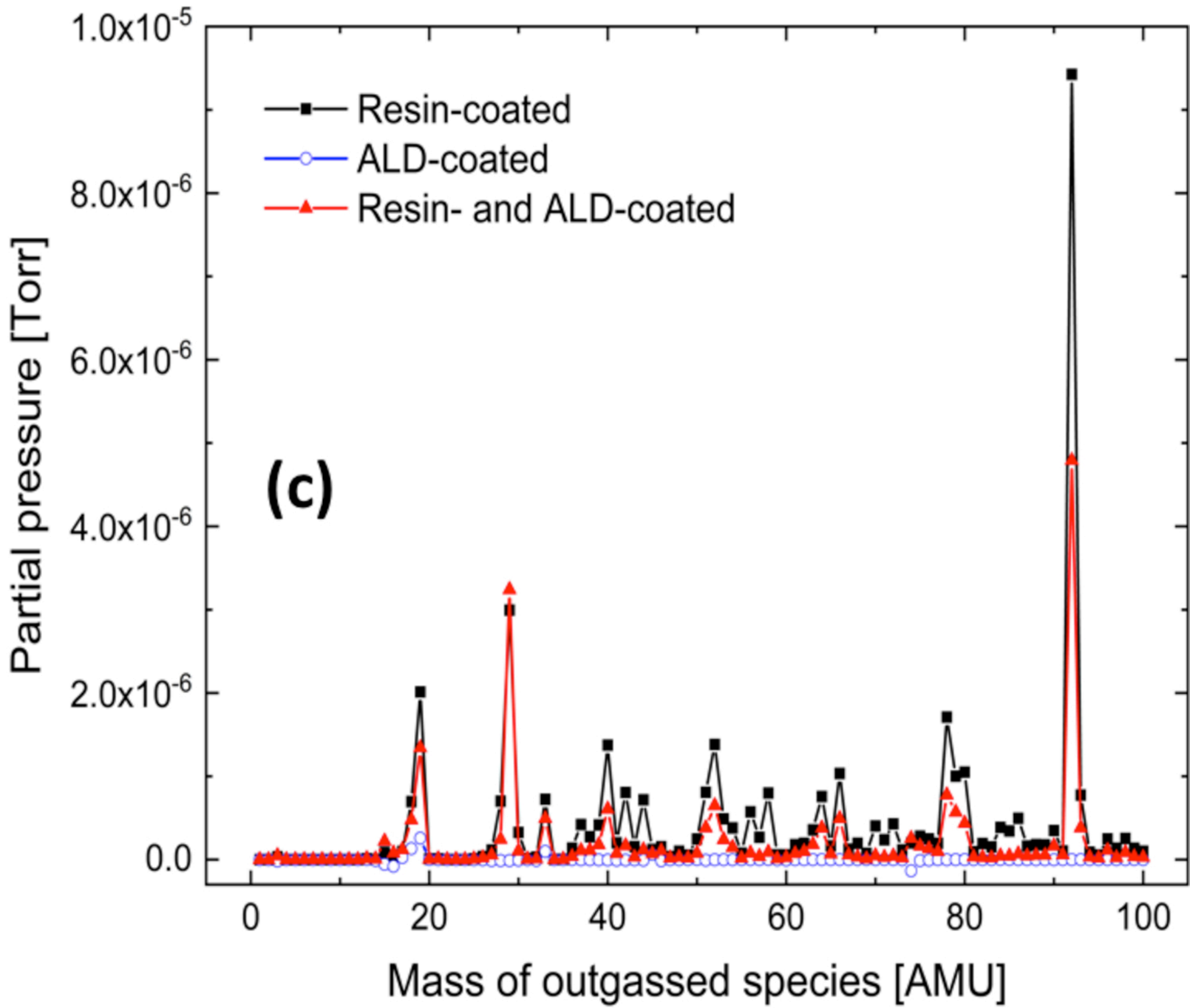
Resin-coated
ALD-coated
Resin- and ALD-coated
(c)
Partial pressure [Torr]
1.0x10-5
8.0x10-6
6.0x10-6
4.0x10-6
2.0x10-6
0.0
0
20
40
60
80
100
Mass of outgassed species [AMU]